



# CEMB

## RESEARCH SYMPOSIUM

### UNDERGRADUATES EXPANDING BOUNDARIES

AUGUST 6, 2021 | 1PM-4PM EST

Meeting Link: <https://bit.ly/2021-UEXB-Penn>



- |      |  |   |
|------|--|---|
| 1:00 |  | Welcoming Remarks, Rebecca Wells, CEMB Director of Education  |
| 1:05 |  | The Effect of Modulating HIF and YAP on Metabolic Activity of Murine Periosteal Cells In Vitro<br><b>Mística Lozano Perez, University of Texas at San Antonio</b><br>Boerckel Lab                                   |
| 1:17 |  | Role of Actin Stress Fibers and Rho Signaling on Chondrogenic Gene Expression in ATDC5 cells as a Function of Substrate-Stiffness<br><b>Diana Cruz Garcia, University of California Merced</b><br>Mauck Lab         |
| 1:29 |  | A Computational Analysis of Inertial Loading on the Brain<br><b>Noah Kim, Auburn University</b><br>Shenoy Lab   |
| 1:41 |  | Predicting the Turgor Pressure-Driven Mechanical Interactions of Guard and Pavement Cells During Stomatal Opening in Plants<br><b>Mythili Subbanna, Amherst College</b><br>Anderson Lab                             |
| 1:53 |  | Cell wall patterning in Arabidopsis thaliana roots is influenced by the mechanical environment in agar and a hydrogel-based transparent soil<br><b>Matthew Egner, Pennsylvania State University</b><br>Anderson Lab |
| 2:05 |  | Synthesis, Characterization, and Flow Behavior of Biomaterial-based Microfibers<br><b>Kaitlyn McHugh, University of Pittsburgh</b><br>Osuji Lab   |
| 2:17 |  | Actomyosin and Oxidative Stress's Effect on Heart Beating and Cell Genome Expression<br><b>Elizabeth Seidl, Kansas State University</b><br>Discher Lab  |
| 2:29 |  | Modeling of Hydrolytically Degradable, Thiol-Ene Crosslinked Hyaluronic Acid Hydrogels<br><b>Bruce Enzmann, Johns Hopkins University</b><br>Burdick Lab   |
| 2:41 |  | Relating Cell Type Identification to Label-Free Collagen and Myosin Measures in Developing Heart<br><b>Nathan Rojas Ocampo, Columbia University</b><br>Discher Lab  |



2:53	Update on Viscoelastic Properties of Tofu as a Phantom for Liver Disease Diagnosis <b>Katherine Kerr, Purdue University</b> Janmey Lab
3:05	Varying Mechanics and Structure of Polyacrylamide Pillars, a Model for the Bile Duct <b>Zina Helal, University of Texas at San Antonio</b> Wells Lab
3:17	Application of conductive Chitosan-Polyaniline Composite Scaffold for Tissue Engineering <b>Emily Rudolph, Widener University</b> Janmey Lab
3:29	Understanding the Role of Microenvironmental Curvature on Cholangiocyte Behavior <b>Elaine Nagahara, Johns Hopkins University</b> Wells and Stebe Labs
3:41	Mechanical Basis of Kidney Branching Morphogenesis <b>Marysol Chu Carty, The City College of New York, &amp; Michael Foster, Community College of Philadelphia</b> Hughes Lab
3:55	Closing Remarks

## Abstracts

### The Effect of Modulating HIF and YAP on Metabolic Activity of Murine Periosteal Cells In Vitro

**Mistica Lozano Perez**, Madhura Nijsure, Annemarie Lang, Joel D. Boerckel



After bones undergo fractures, multiple pathways activate to aid the bone to regenerate. These pathways involve both mechanical and chemical stimuli. One pathway is known as the HIF pathway and is characterised by activating in response to low oxygen levels in the environment. This pathway occurs because bone fracturing is accompanied with a disturbance in blood vessels surrounding the site of injury, and thus, a loss of oxygen. During this regeneration process, mechanical cues are known to induce two downstream regulators of the HIPPO pathway: Yes-associated protein (YAP) and TAZ. These regulators aid in cell proliferations and are activated by mechanical cues. Both the HIF and HIPPO pathways activate parallel to each other, so we tested whether they interact with one another by first using small molecules to induce or inhibit HIF or YAP in vitro.

Initial results indicated that Deferoxamine (DFO: HIF stabilizer) affected cellular metabolic activity more than other test groups. Following this experiment, we tested the DFO in different concentrations to observe the cellular response to a gradually decreasing concentration of DFO. These results indicated to us that DFO and therefore HIF strongly modulate the metabolic activity of periosteal cells in vitro. Future experiments will focus more on the precise mechanisms that underlie these observations and the possible interactions between this pathway and the HIPPO signaling pathway.

### Role of Actin Stress Fibers and Rho Signaling on Chondrogenic Gene Expression in ATDC5 cells as a Function of Substrate-Stiffness

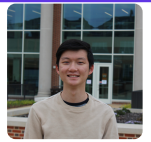
**Diana Cruz Garcia**, Ryan Daniels, Robert Mauck



Articular chondrocytes (ACs) are the sole cell type in articular cartilage. These cells produce the matrix that enables a high compressive modulus and a smooth surface for near-frictionless movement. In healthy ACs, actin filaments are separated from the nucleus in a cortical-like organization and express transcription factors Sox9, Collagen 2 (Col 2), and Aggrecan. However, in diseased/dedifferentiated ACs, numerous large actin stress fibers form that engage the nucleus and there is a consequent decrease in chondrocyte-specific gene expression. Increases in canonical Rho signaling leads to the formation of actin stress fibers which results in a decrease of chondrogenic gene expression. Here, we explore the influence of different substrate stiffnesses on ATDC5 cells chondrogenic gene expression when treated with Rho inhibitors/activators and actin stress fiber promoters. ATDC5 cells were seeded on fibronectin-coated polyacrylamide (PA) gels to test the effects of substrate stiffness (glass, 55 kPa, 5 kPa). Small molecules (LPA: Rho agonist, CT04: Rho inhibitor, Jasplakinolide (Jsp): f-actin promoter) were added and RNA was isolated to assay for changes in gene expression using qPCR. We observed that a decrease in substrate stiffness led to a significant increase in chondrogenic gene expression. Our results support a causal link to decreasing substrate stiffness and actin stress fiber formation with increased chondrogenic gene expression. We found that increasing either Rho signaling, or actin stress fiber formation decreased chondrogenic gene expression on soft substrates. These results could suggest that actin stress fiber formation initiates chondrocyte dedifferentiation when chondrocytes are in a diseased or damaged environment.

## A Computational Analysis of Inertial Loading on the Brain

Noah Kim, Aayush Kant, Vivek Shenoy



Computational brain models allow for safe and cost-effective simulation of traumatic brain injury (TBI). However, brain models must include key features to produce accurate results. Brain properties such as anisotropic white matter and ventricles contribute to concentrated areas of shear stress around the ventricular region. Shear stress along neural tracts causes diffuse axonal injury (DAI) in which axons stretch and lose biochemical processes required for regular function, resulting in cell impairment or death. The purpose of this study was to build upon previous TBI experiments and better understand the results of including key brain structures and properties during inertial loading. Data taken from a diffusion tensor imaging (DTI) experiment for a coronal cross-section of the brain was processed using MATLAB to outline the outer boundary of the brain, interface between grey and white matter, and ventricles. Vectors denoting axon tract direction in white matter were filtered to reveal white matter anisotropy. To examine how much the presence of ventricles affected simulated force distribution, multiple models combining or excluding certain factors were created in COMSOL. Material properties from a previous study were used to model the gray matter, white matter, and intraventricular cerebrospinal fluid. Rapid rotational acceleration and deceleration are predicted to contribute greatest towards DAI, so a time-dependent rotational study using a triangular impulse model with max angular velocities ranging from 20 to 200 rad/s was run on each model. Simulation results revealed that high-stress areas were concentrated at the corners of ventricles. Future work will focus on implementation of white-matter and axon tracts into the model.

## Predicting the Turgor Pressure-Driven Mechanical Interactions of Guard and Pavement Cells During Stomatal Opening in Plants

Mythili Subbanna, Yintong Chen, Hojae Yi, Eoin McEvoy, Charles T. Anderson



Stomata are tiny pores on the plant surface that regular gas exchange and thus photosynthesis and transpiration. In *Arabidopsis thaliana*, stomatal complexes comprise two kidney-shaped guard cells and are surrounded by pavement (epidermal) cells. Stomatal opening and closure are determined by ion and water fluxes into and out of guard cells, and their subsequent effects on turgor pressure and cell volume. However, the three-dimensional dynamics of guard and pavement cells during stomatal opening are still unclear, leaving us with an incomplete picture of stomatal mechanics. Previously, we found that during stomatal opening, guard cells increase in XY area while neighboring pavement cells show no significant change in area. Here, we hypothesized that mechanical interactions between guard and pavement cells affects the efficiency of stomatal opening. To understand how guard and pavement cells mechanically interact during stomatal opening, a 3D stomatal complex model was created and analyzed using Finite Element Modeling, a computational method to obtain an approximate solution to governing models for systems with complex geometry under defined constraints. This model encompasses the anisotropic expansion and volume changes of guard cells during stomatal opening. Currently, result generation is in progress. Greater guard to pavement cell turgor pressure ratios resulting in larger increases in stomatal complex width would indicate that efficient stomatal opening depends on the guard cell pushing into the pavement cells. Simulated ablation, or removal, of pavement cells, is expected to allow for further opening of the stomata, supporting the idea that pavement cell presence plays a large mechanical role in proper stomatal opening. We are currently working to place results from our modeling work in the context of underlying ion and water fluxes to understand how cells respond and adapt to their mechanical environment to allow for stomatal function.

## Cell wall patterning in *Arabidopsis thaliana* roots is influenced by the mechanical environment in agar and a hydrogel-based transparent soil

Matthew R. Egner, Oskar Siemianowski, Charles T. Anderson



Little is known about the mechanobiology of cell wall patterning in plants. Understanding how roots and cell walls respond to the mechanical environment on the cellular level can provide insights for enhancing plant growth and crop yields. We hypothesized that roots encountering harder media will remodel their cell walls and have different cellulose patterning than roots grown on the surface of or inside softer media. Wild-type *Arabidopsis thaliana* seedlings were grown on the surface of 0.8% (w/v) agar and inside various concentrations of agar and a hydrogel-based transparent soil composed of alginate/phytagel beads. After 6 days, roots were removed and stained for high-resolution imaging of cell walls with confocal microscopy. ImageJ was used to analyze cellulose orientations. We found that roots grown on the surface of 0.8% (w/v) agar had more deviation of cellulose orientations and a lower anisotropy than those inside 0.8% (w/v) agar. Roots grown inside 0.4% (w/v) agar had less deviation in cellulose orientation and higher anisotropy when compared to those inside 0.8% (w/v) agar. Roots grown in transparent soil composed of 0.8% (w/v) beads contained higher anisotropy than those grown on the surface of agar and in 1.2% (w/v) beads, while those in 0.7% (w/v) beads had the least anisotropy. Together, these results indicate that growing roots inside media might constrain cellulose fibril orientation more than growing roots on an agar surface. When comparing agar concentrations, there was a higher alignment of cellulose in the softer agar than in hard, but in transparent soil, the softest beads had the least aligned fibrils. Future research includes collecting high-resolution in vivo images of cell walls for roots grown inside various mechanical strengths of transparent soil without removing the seedlings for staining.



## Synthesis, Characterization, and Flow Behavior of Biomaterial-based Microfibers

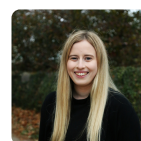
**Kaitlyn McHugh**, Ravisara (Ning) Wattana, Chinedum Osuji



Microfibers are a unique class of materials because properties like mechanical strength, elasticity, length, and diameter can be controlled during synthesis, which has led to their use in biological processes like drug delivery and tissue engineering. Synthetic polyacrylonitrile (PAN) fibers are often used due to their strong mechanical properties, but they are less biocompatible than natural substances like cellulose nanofibers and alginate. The goal of this study is to investigate the synthesis, characterization, and flow behavior of nanocellulose and alginate-based fibers and compare with PAN fibers. The fibers were prepared by wet spinning precursor solutions into a coagulation bath of nonsolvent. 3% wt PAN was dissolved in dimethylformamide and extruded into water. Various ratios of alginic acid (AA) to cellulose nanofibers (CNF) were prepared by dissolving in water and extruding into 5% wt CaCl<sub>2</sub>. The morphology of the fibers were investigated under optical microscope and scanning electron microscope. Mechanical properties of the precursors and extruded fibers, including viscosity and tensile strength were analyzed with rheometer. Our results show that fibers in the target range of 17 to 181  $\mu\text{m}$  can be synthesized for most precursor solutions, but mixtures of AA and CNF were more challenging, as the diameter of the CNF-based fibers was more likely to deviate from the size of the extrusion needle. Adding CNF to the AA solution resulted in non-Newtonian behavior, while other precursors exhibit Newtonian behavior. This indicates that many factors determine the characteristics of the final fibers, including flow behavior, extrusion pathway, and extrusion rate.

## Actomyosin and Oxidative Stress's Effect on Heart Beating and Cell Genome Expression

**Elizabeth Seidl**, Manasvita Vashisth, Karanvir Saini, Mai Wang, Manu Tewari, Dennis Discher



DNA damage within the cell is increases due to mislocalization of the DNA repair factors leading to accumulation of DNA damage, premature aging, cell cycle arrest and aberrant heart beating. Single cell sequencing allows us to look at the different cell types within embryonic chick hearts and compare their genome expression. Understanding acto-myosin stress and DNA damage's relationship with aberrant beating, cell cycle arrest and the cellular genome can help us better understand what cell types are most susceptible to DNA damage, and eventual possible premature aging. Hearts were treated with four experimental groups: blebbistatin, blebbistatin + washout, DMSO, and H<sub>2</sub>O<sub>2</sub> to induce oxidative and actomyosin stress. Genomic UMAPs were then created using the Seurat package within R, to visualize genomically similar cell clusters, while biomarker genes were used to identify cell types. A wilcox differential gene expression test was run to compare gene mitotic cell cycle genes. Both CENPF and SMC2 were found to be significantly downregulated in the experimental group H<sub>2</sub>O<sub>2</sub> indicating that DNA damage caused by oxidative stress can cause cell cycle arrest. Blebbistatin treatment was found to alter both beating strain and beating frequency of hearts. Using label-free second harmonic generation (SHG) imaging method, collagen and myosin levels measurements were determined within heart tissue samples in order to compare the acto-mysosin stress effects and ECM collagen levels. compared to DMSO. Label free SHG imaging method produced stronger signal in forward direction as compared to backward direction for myosin fibers present within heart tissues.

## Modeling of Hydrolytically Degradable, Thiol-Ene Crosslinked Hyaluronic Acid Hydrogels

**Bruce P. Enzmann III**, Jonathan H. Galarraga, Abhishek P. Dhand, Nikolas Di Caprio, Jason A. Burdick



Degradable hydrogels have been developed for a range of biomedical applications, including model culture platforms to investigate cellular perception and response to extracellular microenvironments, the delivery of therapeutic molecules, and the engineering of tissues. Towards their use, further characterization and modeling of degradable hydrogels is needed, particularly for those that undergo hydrolytic degradation. To address this, hyaluronic acid (HA) hydrogels that undergo tunable hydrolysis were fabricated. HA was first reacted with variable concentrations of carbic anhydride to obtain norbornene-modified HA (NorHACA) with hydrolytically labile pendant groups. NorHACA (14, 30, or 40% modification) was then mixed with photoinitiator and di-thiol crosslinker and crosslinked via thiol-ene photocrosslinking. The storage and compressive moduli of NorHACA hydrogels could be readily tuned via changes in polymer concentration, crosslinker concentration, and degree of modification. To characterize bulk degradation, hydrogels were incubated in phosphate buffered saline at 37 °C, the supernatant was collected over time, and degradation profiles were constructed using a 96-well uronic acid assay. Rate constants describing NorHACA hydrolysis were then extrapolated from degradation profiles by assuming pseudo-first order degradation kinetics and performing exponential curve fits. Thereafter, we developed a MATLAB model to predict hydrogel disintegration times and bulk degradation behavior from gel composition and degradation kinetics. NorHACA hydrogels exhibit modular mechanical properties and degradation behavior, demonstrating promise for future applications in tissue engineering and biofabrication. Further development of our model will simulate the degradation of hydrogels composed of multiple polymers, such that hydrogels may be designed with user-defined mechanical properties and disintegration times.

## Relating Cell Type Identification to Label-Free Collagen and Myosin Measures in Developing Heart

**Nathan Rojas Ocampo**, Karanvir Saini, Manasvita Vashisth, Mai Wang, Dennis Discher



Lamin-A is an important protein that has been previously identified as a mechanosensitive protein located under the nuclear membrane that protects cells from DNA damage. It scales with collagen, the most abundant protein in the extracellular matrix (ECM), which also determines tissue stiffness. Low levels of lamin-A paired with constant acto-myosin stress, leads to increased DNA damage due to mislocalization of DNA repair factors. Accumulation of DNA damage in the cell along with telomere shortening may lead to premature aging. Additionally, DNA damage can cause cell cycle arrest and aberrant heart beating in developing hearts. Alterations in the acto-myosin stress within cells of the embryonic chick hearts can be made pharmacologically using blebbistatin, a myosin inhibitor, that ultimately leads to altered beating patterns of the hearts and stress on ECM collagen. Single cell RNA sequencing (scRNA-seq) provides high resolution gene expression of the hearts which enables cell type clustering, comparison of mechanosensitivity, and identification of DNA damage levels to understand which cell types are most mechanosensitive and susceptible to DNA damage due to low levels of lamin-A.

## Update on Viscoelastic Properties of Tofu as a Phantom for Liver Disease Diagnosis

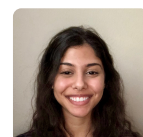
**Katherine Kerr**, Paul Janmey



Liver disease is the cause of approximately two million deaths globally each year. Many liver diseases, such as liver fibrosis, are characterized by alterations in the mechanical properties of liver tissues. Magnetic resonance elastography (MRE), a method that combines magnetic resonance imaging (MRI) with mechanical stimulation, provides a noninvasive tool to diagnose and monitor liver disease by measuring the mechanical properties of tissues. To ensure accurate evaluations of tissue properties, materials called phantoms are often used to calibrate an MRI device. Traditional phantoms lack complex structures associated with liver tissue. Tofu offers a phantom candidate that has been shown to reflect the materials properties of liver in MRE better than currently available phantoms designed for MRI. In this work, the rheological properties of commercial tofu were studied at different frequencies using a home-made torsion pendulum. The pendulum was compromised of a ruler sandwiched between two aluminum plates, a labjack to which the tofu was fixed, and a rotary motion sensor. A cylindrical tofu sample was sandwiched between the labjack and plates. Weights were added to the ends of the ruler to change the frequency. The plates were rotated by a small angle and then released. The subsequent oscillation angle was measured and used to compute the viscoelastic properties of tofu over a range of 0.5 Hz to 2 Hz. It was found that tofu exhibited frequency dependent properties, being qualitatively similar to liver properties. Our results suggest that tofu could be used as a tissue mimicking phantom to calibrate and validate MRE results.

## Varying Mechanics and Structure of Polyacrylamide Pillars, a Model for the Bile Duct

**Zina Helal**, David Li, Rebecca G. Wells



Biliary atresia (BA) is a neonatal disease in which bile ducts become fibrotic and can lead to cirrhosis and death within the first years of life if left untreated. Little is understood about BA pathogenesis, but it is likely that ducts become stiffer as fibrosis develops, which may be a key factor affecting cell mechanics and associated disease development. To further understand how stiffened bile duct tissues may affect behavior of the mesenchymal cells surrounding the lumen, we developed an in-vitro polyacrylamide (PA) hydrogel model of the bile duct. We hypothesized that by varying the stiffness and curvature of PA pillars, fabrication can be optimized to model normal and obstructed interlobular and septal bile ducts. An array of polyacrylamide gel micro-pillars was fabricated through an adapted mold-pattern transfer process. Photolithographic techniques were optimized to generate SU-8 photoresist silicon molds containing holes 500  $\mu\text{m}$  in depth with diameters of 75  $\mu\text{m}$  and 300  $\mu\text{m}$ . PA gels with stiffness chosen to mimic those of normal and obstructed bile ducts (1.1 kPa, 3.1 kPa and 14 kPa) are polymerized over the molds using UV photoinitiation. Pillar geometry measured with epi-fluorescent microscopy verified physiologically relevant formation of micro-pillars with height up to 400  $\mu\text{m}$ . Future cell studies seeding gallbladder fibroblast on the pillars will characterize cell phenotype and alignment as a function of pillar stiffness and curvature. This will provide greater insight into how cells sense and respond to stiffened ducts from the smallest parts of the biliary tree and will further our understanding of possible cellular mechanisms involved in BA pathogenesis.





## Application of conductive Chitosan-Polyaniline Composite Scaffold for Tissue Engineering

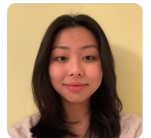
Emily Rudolph, Paul Janmey



Multiple reports in the nerve tissue engineering field have revealed that electrical stimulation (ES) within conductive polymer substrates can significantly influence stem cell behaviors such as, proliferation, morphology, and differentiation. Therefore, it is essential to characterize the effects of electroconductive substrates and electric field stimuli on stem cell fate processes to improve stem cell-based regenerative therapies. In this study, we developed a Chitosan-polyaniline composite scaffold as a conductive platform for tissue engineering applications. We synthesized a conductive composite polymer based on chitosan-polyaniline (CS-PANI). Then, using the prepared copolymer, a conductive hydrogel film was fabricated by the gel casting technique. Also, Chitosan hydrogel film was prepared as a control sample. After, we used the Fourier Transform Infrared (FTIR) Spectroscopy for the characterization of the physicochemical properties of the prepared hydrogels and measurement of electrical conductivity. In the next step, human mesenchymal stem cells (hMSCs) were seeded on these scaffolds and the ES was applied to the conductive scaffold to establish an electrical environment to manipulate the cells seeded on it. Then, the effects of ES on cell viability, morphology and proliferation were examined. The F-actin staining results showed that the scaffold with polyaniline, and chitosan create an elongation of the cell while the chitosan scaffold did not have as prominent of an effect. The obtained results of viability display a high percentage of the seeded cells surviving under ES. Therefore, suggesting the combination of CS and CS-PANI with ES has great compatibility with hMSCs.

## Understanding the Role of Microenvironmental Curvature on Cholangiocyte Behavior

Elaine A. Nagahara, Kapish Gupta, Jed-Joan S. Edziah, Jiayi Deng, Kathleen J. Stebe, and Rebecca G. Wells



Studies on cell migration and morphology are often done on planar surfaces even though their environment is geometrically complex. In the body, there are various glands that have unique geometries with specific Gaussian curvatures. However, their effects on cell behaviors are not well understood in part due to the difficulty of replicating environmental curvature. Here, using surface tension properties, we developed two curvature models based on particles of different sizes. Collagen poured over the particles formed spherical caps at the top with positive Gaussian curvature and skirts at the bottom with negative Gaussian curvature. Cholangiocytes were then seeded to investigate how such curvature influences cell migration and morphology. We optimized these models to address three fabrication issues: collagen detachment, collagen contraction, and small particle detachment. Preliminary results show that we fabricated models with collagen-substrate contact angle  $\theta = 12.04^\circ$  and  $10.87^\circ$  and particle-collagen contact angle  $\phi = 21.92^\circ$  and  $24.35^\circ$  for the larger and smaller structures respectively. In the larger models, cells were seen protruding and migrating at least 250  $\mu\text{m}$  ( $>10\times$  cell diameter) towards the spherical cap. The cells towards the top displayed circularity and aspect ratio 15% lower and 32% higher, respectively, relative to cells towards the bottom. As epithelial cells attach and move, they become less circular and more morphologically fibroblastic, supplementing the idea that the cells towards the top needed to form more adhesions to stabilize their positions on a slope and form protrusions to migrate. Observing how cells may have migratory preferences for certain curvatures provides insight into controlling cell organization, especially for simulating glands that naturally have Gaussian curvature.



## Mechanical Basis of Kidney Branching Morphogenesis

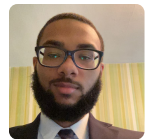
Marysol Chu Carty, Michael Foster, Aria Huang, Nathan Petrikas, John Viola, Alex Hughes



Branching morphogenesis in the embryonic kidney leads to the formation of the urinary collecting system. Defective branching can lead to complications such as a lack of one or two kidneys, hypoplasia, or higher risk of adult diseases including hypertension. Branching begins with the invasion of the Wolfian duct into the surrounding mesenchymal tissue leading to the development of a tree-like structure. As this process continues, cap mesenchyme cells epithelialize and mature into nephrons in the “armpit” region of the branching tips. Glial cell derived neurotrophic factor (GDNF), is produced by the cap mesenchyme and promotes ureteric bud (UB) migration by binding and activating Ret, a transmembrane receptor that is present in the UB. The Ret-activated cells at the tips of the UB are more motile and responsible for branching. The trunk cells, which are not Ret-activated are less motile and provide structural support for the ureteric tree; however, the mechanical differences in UB cells due to Ret signaling is not fully understood. We investigated how Ret activation affects the forces exerted by ureteric bud-like cells to understand how branching morphogenesis of the UB sculpts the mechanical environment of the developing kidney. Madin-Darby Canine Kidney (MDCK) cells that were transfected with the Ret gene to express the receptor were used to model the UB. These cells were plated on a 4% T and 2.6% C polyacrylamide gel which was embedded with fluorescent beads. The gel was then functionalized with fibronectin to promote cell adhesion. GFR $\alpha$ -1 and GDNF were used to activate the Ret signaling pathway in one group of cells and contractility was compared to cells in basal media. The cells were imaged using confocal microscopy before and after trypsinization to measure bead displacement. The data that was collected was analyzed and used to generate a vector force map. Based on analysis results from published software, MDCK cells with activated Ret exhibited greater displacement of the beads in the gel and therefore exerted a larger force in the leading and trailing edges of the cell. Our data may contribute new insights into the mechanical effects of GDNF signaling in the developing kidney. In addition to the established roles of GDNF activation in cell motility, it could also mediate intracellular forces and local ECM remodeling as evidenced by higher traction strains measured in our polyacrylamide substrates.

## Effects of RET and GDNF to the mechanical environment of the ureteric bud during kidney branching morphogenesis

Michael Foster, Marysol Chu, John Viola, Zheyuan (Aria) Huang, Nathan Petrikas, Alex Hughes



Branching Morphogenesis (BM) contributes to kidney development where the ureteric bud (UB) and metanephric mesenchyme (MM) form by the UB budding into the MM to begin a growing and branching process into a mature ureteric collecting duct. RET and GDNF are two signaling proteins that help direct this process in the kidney. RET is a receptor located on the surface of the UB which has high activity at the tip and has low activity in the trunk of the UB. The high activity of RET in the tip of the UB causes it to be more motile leading it towards the MM which produces GDNF which is a chemoattractant to lead the outgrowth and branching of the UB. Abnormalities to the mechanical environment can lead to defects to the growth and branching of these structures which can result in congenital defects such as renal agenesis, hypoplasia, or congenital obstructive uropathy. These congenital defects could be attributed to the lack of these two signaling proteins causing abnormalities to the mechanical environment. To understand how RET and GDNF affect how the UB cells extracellular mechanical properties impact BM, we used Madin-Darby canine kidney cells (MDCK) an immortalized cell line that are morphologically similar to the renal distal tubular epithelium which in the kidney has high RET expression. The MDCK cells used have been engineered to express RET is known for increasing MDCK cell motility and migration towards a localized source of GDNF ; so the focus is on how RET and GDNF impacts the cells contractility on substrate. Thus, understanding how RET and GDNF affect the contractility of MDCK cells will help give insight on how this interaction affects the mechanical environment and UB growth during BM in the kidney. This can then lead to finding possible methods to clinically treat the defects and abnormalities associated with BM. 2,500 MDCK cells were seeded on a 4%C bis-acrylamide and 2.6%T acrylamide polyacrylamide gel (PA) that is 30 micrometers in height on top of a microscope slide. PA gels were prepared with a 1/10k concentration of fluorescent microbeads. The gel and slide were assembled in an 8-well cell culture chamber. For adherence, gels were coated with a 100 mg/mL concentration of fibronectin, following the application of sulfo-SANPAH to the gel and then were incubated. MDCKs were seeded onto the gel in DMEM media containing GDNF/Gfra-1 and normal DMEM. Images of the cells before and after being detached with trypsin were taken. Fiji plugin iterative PIV was used to measure and analyze the displacement of the beads, followed by FTTC plugin used to obtain a displacement map. We compared RET transformed MDCK cells with MDCK cells that do not express the RET receptor. The MDCK RET cells expressed greater contractility and adhesion when in GDNF/Gfra-1 media. This was shown when the cells were on the PA gel where they displayed high displacement of the fluorescent microbeads. These results suggest that GDNF and RET impact the ability of MDCK cells to contract. Lastly, these findings contribute to the understanding of how RET and GDNF impact the contractility of UB cells inside of the kidney contributing to the mechanical process of branching morphogenesis.

